Progress of Theoretical Physics, Vol. 128, No. 1, July 2012

Structure of ${}^{10}_{\Lambda}$Be and ${}^{10}_{\Lambda}$B Hypernuclei Studied with the Four-Body Cluster Model

Emiko Hiyama and Yasuo Yamamoto

Nishina Center for Accelerator-Based Science, Institute for Physical and Chemical Research (RIKEN), Wako 351-0198, Japan

(Received March 17, 2012; Revised April 29, 2012)

The structure of the isodoublet hypernuclei, ${}^{10}_{\Lambda}$B and ${}^{10}_{\Lambda}$Be within the framework of an $\alpha+\alpha+\Lambda+N$ four-body cluster model is studied. Interactions between the constituent subunits are determined to reproduce reasonably well the observed low-energy properties of the $\alpha\alpha$, αN, $\alpha\Lambda$, $\alpha\alpha\Lambda$, and $\alpha\alpha N$ subsystems. Furthermore, the two-body ΛN interaction is adjusted to reproduce the 0^+-1^+ splitting of ${}^{4}_{\Lambda}$H. The Λ binding energies of ${}^{10}_{\Lambda}$B and ${}^{10}_{\Lambda}$Be are 8.76 MeV and 8.94 MeV, respectively. The energy splitting of the 1^--2^- levels in ${}^{10}_{\Lambda}$B is 0.08 MeV, which does not contradict the experimental report in BNL-E930. An even-state ΛN charge symmetry breaking (CSB) interaction determined from the $A=4$ systems works repulsively by +0.1 MeV (attractively by −0.1 MeV) in ${}^{10}_{\Lambda}$Be (${}^{10}_{\Lambda}$B). We discuss a possibility that an odd-state CSB interaction improves the fitting to the experimental data of $A=10$ double Λ hypernuclei.

Subject Index: 214

§1. Introduction

One of the primary goals in hypernuclear physics is to extract information about baryon-baryon interactions in a unified way. By making use of the hyperon(Y)-nucleon(N) scattering data and the rich complementary NN data, several types of YN/YY interaction models have been proposed, which are based on the $SU(3)$ and $SU(6)$ symmetries. However, these YN/YY interaction models have a great deal of ambiguity at present, since the YN scattering experiments are extremely limited and there is no YY scattering data. Therefore, it is important to extract useful information on YN/YY interactions from studies of hypernuclear structures. In the case of the ΛN sector, the results of high-resolution γ-ray experiments have been quite important for such a purpose, where level structures of Λ hypernuclei are determined within keV systematically.

Theoretically, a powerful calculation method, the Gaussian Expansion Method (GEM),[1] was proposed as a means of performing accurate calculations of the structure for three- and four-body systems. GEM has been used to successfully study structures for a variety of few-body systems in atomic, baryonic and quark-level problems. In order to extract information about the ΛN interaction, this method was applied to s- and p-shell Λ-hypernuclei represented by three- and/or four-body models composed of Λ and nuclear-cluster subunits, and the spin-dependent parts of the ΛN interactions were determined using the results of the γ-ray experiments. In Ref. 2), the ΛN spin-orbit interactions were determined from the observed energies of spin-doublet states in ${}^{9}_{\Lambda}$Be (${}^{13}_{\Lambda}$C) represented by the $\alpha\alpha\Lambda$ ($\alpha\alpha\alpha\Lambda$) cluster

model. In Ref. 3), the ΛN spin-spin interactions in even- and odd-states were investigated through the combined analyses of ${}^{4}_{\Lambda}$H (${}^{4}_{\Lambda}$He) and ${}^{7}_{\Lambda}$Li ($\alpha pn\Lambda$), where the above spin-orbit interaction was used as an input. These works indicate that we are now entering a new stage of extracting detailed information on the ΛN interaction by combining few-body calculations and γ-ray experimental data.

In this work, on the basis of our previous studies, we investigate structures of ${}^{10}_{\Lambda}$Be ($\alpha\alpha n\Lambda$) and ${}^{10}_{\Lambda}$B ($\alpha\alpha p\Lambda$) and properties of the underlying ΛN interaction. These Λ hypernuclei have provided us many interesting insights so far. For example, aiming to study ΛN spin-dependent interactions, the high-resolution γ-ray experiment was performed to measure the splitting of the 1^--2^- levels of ${}^{10}_{\Lambda}$B in BNL-E930.[4] However, they observed no γ transition between the ground state doublet: This suggests that the 1^--2^- energy splitting in ${}^{10}_{\Lambda}$B is less than 100 keV, or the ground state of this hypernucleus is a 2^- state.

In order to explain the energy splitting in this hypernucleus, the shell model calculation including ΛN-ΣN coupling explicitly was performed by Millener,[5] where observed spectra of p-shell hypernuclei were reproduced systematically with the five parameters giving $p_N s_\Lambda$ two-body matrix elements. When this analysis was applied straightforwardly to ${}^{10}_{\Lambda}$B, they obtained the ground 1^- state and the 1^--2^- splitting energy of 120 keV.[6] This splitting is slightly larger than the above limitation energy of 100 keV to observe the M1 transition from the 2^- state to the 1^- state. They also showed that another interaction set could give rise to the much smaller value of 34 keV[6] and they mentioned that the $\Lambda\Sigma$ coupling interaction in this case was unrealistic. Thus, it is not so simple to reproduce the splitting energy of less than 100 keV in the shell model analysis. It is very important to investigate the level structures of ${}^{10}_{\Lambda}$Be and ${}^{10}_{\Lambda}$B within the framework of the $\alpha\alpha N\Lambda$ four-body cluster model. It is reasonable to employ the $\alpha\alpha N\Lambda$ four-body model, since the core nuclei ^{9}B and ^{9}Be are well described by using $\alpha\alpha N$ three-body cluster model, and, therefore, it should be possible to model the structure change of ^{9}B and ^{9}Be owing to the addition of one Λ particle as a four-body problem.

Another interesting insight is related to the charge symmetry breaking (CSB) components in the ΛN interaction. It is considered that the most reliable evidence for CSB appears in the Λ binding energies B_Λ of the $A = 4$ members with $T = 1/2$ (${}^{4}_{\Lambda}$He and ${}^{4}_{\Lambda}$H). Then, the CSB effects are attributed to the differences $\Delta_{CSB} = B_\Lambda({}^{4}_{\Lambda}\mathrm{He}) - B_\Lambda({}^{4}_{\Lambda}\mathrm{H})$, the experimental values of which are 0.35 ± 0.06 MeV and 0.24 ± 0.06 MeV for the ground (0^+) and excited (1^+) states, respectively.

The pioneering idea for the origin of the CSB interaction was given in Ref. 7), where Λ-Σ^0 mixing leads to an OPEP-type CSB interaction. This type of meson-theoretical CSB model was shown to yield a Δ_{CSB} value for the 0^+ state in ${}^{4}_{\Lambda}$He and ${}^{4}_{\Lambda}$H more or less consistent with the experimental value. Such interactions, however, could not reproduce the Δ_{CSB} value for the 1^+ state.[8),9)]

The CSB effect is generated also by treating the masses of $\Sigma^{\pm,0}$ explicitly in $(NNN\Lambda)$+$(NNN\Sigma)$ coupled four-body calculations of ${}^{4}_{\Lambda}$He and ${}^{4}_{\Lambda}$H. In modern YN interactions such as the NSC models,[10),11)] both elements of the Λ-Σ^0 mixing and the mass difference of $\Sigma^{\pm,0}$ are taken into account. The exact four-body calculations for ${}^{4}_{\Lambda}$He and ${}^{4}_{\Lambda}$H were performed using NSC89/97e models in Ref. 12). It was shown

here that the CSB effect was brought about dominantly by the $\Sigma^{\pm,0}$ mass-difference effect. The calculated value of $\Delta_{\rm CSB}$ in the 0^+ state was rather smaller than (in good agreement with) the experimental value for NSC97e (NSC89). In the case of the 1^+ states, the Δ_{CSB} value for NSC97e had an opposite sign from the observed value, and there appeared no bound state for NSC89.

Thus, the origin of the CSB effect in ${}^{4}_{\Lambda}$He and ${}^{4}_{\Lambda}$H is still an open question.

As another approach, phenomenological central CSB interactions were introduced in Refs. 9),13) to reproduce the $\Delta_{\rm CSB}$ values apart from the origin of the CSB effect. Our present work is along this line: We introduce a phenomenological central CSB interaction to reproduce the $\Delta_{\rm CSB}$ values of ${}^{4}_{\Lambda}$H and ${}^{4}_{\Lambda}$He, and use this CSB interaction in order to investigate the CSB effects in heavier systems. There exist mirror hypernuclei in the p-shell region such as the $A=7$, $T=1$ multiplet (${}^{7}_{\Lambda}$He, ${}^{7}_{\Lambda}$Li*, ${}^{7}_{\Lambda}$Be), $A=8$, $T=1/2$ multiplet (${}^{8}_{\Lambda}$Li, ${}^{8}_{\Lambda}$Be), $A=10$, $T=1/2$ multiplet (${}^{10}_{\Lambda}$Be, ${}^{10}_{\Lambda}$B), and so on. Historically, some authors mentioned CSB effects in these p-shell Λ hypernuclei.[14),15)]

In the past, accurate estimates of CSB effects in the p-shell region have been of limited consideration, because the Coulomb energies contribute far more than the CSB interaction:[15)] There has been no microscopic calculation of these hypernuclei taking account of the CSB interaction. Recently, in Ref. 3), we have studied for the first time the CSB effects in ${}^{7}_{\Lambda}$He, ${}^{7}_{\Lambda}$Li and ${}^{7}_{\Lambda}$Be within the $\alpha+\Lambda+N+N$ four-body model, and those in ${}^{8}_{\Lambda}$Li and ${}^{8}_{\Lambda}$Be within the $\alpha+t({}^3\mathrm{He})+\Lambda$ three-body model using the phenomenological even-state CSB interaction determined in ${}^{4}_{\Lambda}$He and ${}^{4}_{\Lambda}$H. This CSB interaction leads inconsistency with the observed data for ${}^{8}_{\Lambda}$Li and ${}^{8}_{\Lambda}$Be. Then, as a trial, we introduced an odd-state component of the CSB interaction with an opposite sign to the even-state CSB to reproduce the observed binding energies of ${}^{8}_{\Lambda}$Li and ${}^{8}_{\Lambda}$Be. It is likely that this odd-state CSB interaction contributes to binding energies of $A=7$ and 10 Λ hypernuclei as long as we use the even-state CSB interaction to reproduce the observed binding energies of $A=4$ hypernuclei. Recently, new experimental data for ${}^{7}_{\Lambda}$He by $(e,e'K^+)$ have been reported at the Thomas Jefferson National Accelerator Facility (JLab).[16),17)]

In this work, we study $A=10$ hypernuclei within the framework of an $\alpha+\alpha+N+\Lambda$ four-body model to take account of the full correlations among all the constituent subunits. In Ref. 18), we performed four-body calculations of $\alpha+\alpha+\Lambda+N$ model for ${}^{10}_{\Lambda}$Be and ${}^{10}_{\Lambda}$B with the ΛN spin-spin interaction only. In the present paper, we employ further ΛN spin-orbit and anti-symmetric spin-orbit forces. Two-body interactions among constituent units are chosen to reproduce all the existing binding energies of the subsystems ($\alpha N, \alpha\alpha\Lambda, \alpha\Lambda$, and so on). The analysis is performed systematically for ground and excited states of the $\alpha\alpha N\Lambda$ systems with no more adjustable parameters in this stage, so that these predictions offer important guidance for the interpretation of the upcoming hypernucleus experiments such as the ${}^{10}\mathrm{B}(e,e'K^+)$ ${}^{10}_{\Lambda}$Be reaction at JLab. The CSB effects in binding energies of ${}^{10}_{\Lambda}$B and ${}^{10}_{\Lambda}$Be are investigated in our four-body model using the even-state CSB interaction determined in ${}^{4}_{\Lambda}$He and ${}^{4}_{\Lambda}$H. Furthermore, as a trial, we introduce an odd-state CSB interaction with an opposite sign to the even-state CSB part to reproduce data of $A=7$ hypernuclei, and apply it to the present $A=10$ systems.

In §2, the microscopic $\alpha\alpha\Lambda N$ calculation method is described. In §3, the interactions are explained. The calculated results and discussion are presented in §4. Section 5 is devoted to a discussion of charge symmetry breaking effects obtained for the $A = 10$ systems. The summary is given in §6.

§2. Four-body cluster model and method

In this work, the hypernuclei, ${}^{10}_{\Lambda}$B and ${}^{10}_{\Lambda}$Be, are considered to be composed of two α clusters, a Λ particle, and a nucleon. The core α clusters are considered to be an inert core and to have the $(0s)^4$ configuration, $\Psi(\alpha)$. The Pauli principle between the valence nucleon and the nucleons in α clusters is taken into account using the orthogonality condition model (OCM),[19] as the valence nucleon's wave function should be orthogonal to nucleons in the α cluster.

Nine sets of Jacobian coordinates for the four-body system of ${}^{10}_{\Lambda}$B and ${}^{10}_{\Lambda}$Be are illustrated in Fig. 1, in which we further take into account the symmetrization between the two αs.

The total Hamiltonian and the Schrödinger equation are given by

$$(H - E)\,\Psi_{JM}({}^{10}_{\Lambda}\mathrm{Z}) = 0\ , \tag{2·1}$$

$$H = T + \sum_{a,b} V_{ab} + V_{\mathrm{Pauli}}\ , \tag{2·2}$$

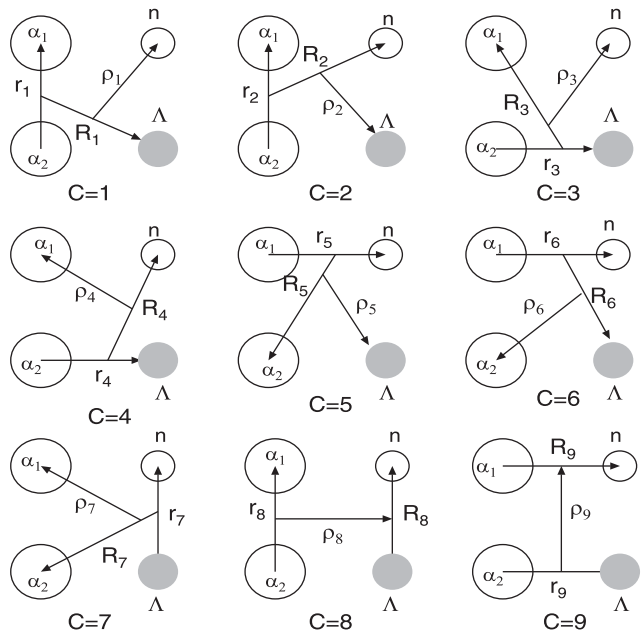

Fig. 1. Jacobi coordinates for all the rearrangement channels ($c = 1 - 9$) of the $\alpha + \alpha + \Lambda + N$ four-body system. Two α clusters are to be symmetrized.

where T is the kinetic-energy operator and V_{ab} is the interaction between constituent particles a and b. The OCM projection operator $V_{\rm Pauli}$ will be given below. The total wavefunction is described as a sum of amplitudes of the rearrangement channels ($c = 1 - 9$) of Fig. 1 in the LS coupling scheme:

$$\begin{aligned}\Psi_{JM}({}^{10}_{\Lambda}\mathrm{Z}) = \sum_{c=1}^{9} \sum_{n,N,\nu} \sum_{l,L,\lambda} \sum_{s,I,K} C^{(c)}_{nlNL\nu\lambda SIK} \\ \times \mathcal{S}_\alpha \Big[\Phi(\alpha_1)\Phi(\alpha_2) \big[\chi_{\frac{1}{2}}(N)\chi_{\frac{1}{2}}(\Lambda) \big]_s \\ \times \big[\big[\phi^{(c)}_{nl}(\boldsymbol{r}_c)\psi^{(c)}_{NL}(\boldsymbol{R}_c) \big]_I \xi^{(c)}_{\nu\lambda}(\boldsymbol{\rho}_c) \big]_K \Big]_{JM} . \end{aligned} \tag{2·3}$$

Here the operator $\mathcal{S}_\alpha$ stands for symmetrization between the two α clusters. $\chi_{\frac{1}{2}}(\Lambda)$ and $\chi_{\frac{1}{2}}(N)$ are the spin functions of the Λ and nucleon, respectively.

Following the Gaussian Expansion Method (GEM),[1),20),21)] we take the functional forms of $\phi_{nlm}(\boldsymbol{r})$, $\psi_{NLM}(\boldsymbol{R})$ and $\xi^{(c)}_{\nu\lambda\mu}(\boldsymbol{\rho})$ as

$$\begin{aligned} \phi_{nlm}(\boldsymbol{r}) &= r^l\, e^{-(r/r_n)^2} Y_{lm}(\widehat{\boldsymbol{r}}) \,, \\ \psi_{NLM}(\boldsymbol{R}) &= R^L\, e^{-(R/R_N)^2} Y_{LM}(\widehat{\boldsymbol{R}}) \,, \\ \xi_{\nu\lambda\mu}(\boldsymbol{\rho}) &= \rho^\lambda\, e^{-(\rho/\rho_\nu)^2} Y_{\lambda\mu}(\widehat{\boldsymbol{\rho}}) \,, \end{aligned} \tag{2·4}$$

where the Gaussian range parameters are chosen according to geometrical progressions:

$$\begin{aligned} r_n &= r_1 a^{n-1}, && (n = 1 - n_{\max}) \\ R_N &= R_1 A^{N-1}, && (N = 1 - N_{\max}) \\ \rho_\nu &= \rho_1 \alpha^{\nu-1}. && (\nu = 1 - \nu_{\max}) \end{aligned} \tag{2·5}$$

The eigenenergy E in Eq. (2·1) and the coefficients C in Eq. (2·3) are determined by the Rayleigh-Ritz variational method.

The Pauli principle between nucleons belonging to two α clusters is taken into account in the orthogonality condition model (OCM).[19)] The OCM projection operator $V_{\rm Pauli}$ appearing in Eq. (2·2) is represented by

$$V_{\rm Pauli} = \lim_{\gamma\to\infty} \gamma \sum_f |\phi_f(\boldsymbol{r}_{\alpha x})\rangle\langle\phi_f(\boldsymbol{r}'_{\alpha x})| \,, \tag{2·6}$$

which rules out the amplitude of the Pauli-forbidden α-α and α-N relative states $\phi_f(\boldsymbol{r}_{\alpha x})$ from the four-body total wavefunction.[22)] The forbidden states are $f = 0S, 1S, 0D$ for $x = \alpha$ and $f = 0S$ for $x = N$, respectively. The Gaussian range parameter b of the single-particle $0s$ orbit in the α cluster $(0s)^4$ is taken to be $b = 1.358$ fm to reproduce the size of the α cluster. In the actual calculations, the strength γ for $V_{\rm Pauli}$ is taken to be 10^4 MeV, which is large enough to push the unphysical forbidden state to the very high energy region, while keeping the physical states unchanged.

§3. Interactions

3.1. *Charge symmetry parts*

For $V_{N\alpha}$, we employ the effective potential proposed in Ref. 23), which is designed so as to reproduce well low-energy scattering phase shifts of the αN system. The Pauli principle between nucleons belonging to the α and the valence nucleon is taken into account in the OCM[19] as mentioned before.

For $V_{\Lambda N}$, we employ the same ΛN potential as that used in the structure calculations of $A = 7$ hypernuclei in Refs. 3) and 24). Namely, this is an effective single-channel interaction simulating the basic features of the Nijmegen model NSC97f,[11] where the ΛN-ΣN coupling effects are renormalized into ΛN-ΛN parts: We use three-range Gaussian potentials designed to reproduce the ΛN scattering phase shifts calculated from NSC97f, with their second-range strengths in the ${}^3E$ and ${}^1E$ states adjusted so that the calculated energies of the 0^+-1^+ doublet state in the $NNN\Lambda$ four-body system are chosen to reproduce the observed splittings of ${}^4_\Lambda$H. Furthermore, the spin-spin parts in the odd states are tuned to yield the experimental splitting energies of ${}^7_\Lambda$Li. The symmetric LS (SLS) and anti-symmetric LS (ALS) parts in $V_{\Lambda N}$ are chosen so as to be consistent with the ${}^9_\Lambda$Be data: The SLS and ALS parts derived from NSC97f with the G-matrix procedure are represented in the two-range form, and then the ALS part is enhanced to reproduce the measured $5/2^+$-$3/2^+$ splitting energy in the $2\alpha + \Lambda$ cluster model.[2]

The interaction $V_{\alpha\Lambda}$ is obtained by folding the ΛN G-matrix interaction derived from the Nijmegen model F(NF)[25] with the density of the α cluster,[26] its strength being adjusted to reproduce the experimental value of $B_\Lambda({}^5_\Lambda\mathrm{He})$. Furthermore, we use $\alpha\Lambda$ SLS and ALS terms, which are obtained by folding the same ΛN SLS and ALS parts as mentioned before.

For $V_{\alpha\alpha}$, we employ the potential that has been used often in the OCM-based cluster-model study of light nuclei.[27] The potential reproduces reasonably well the low-energy scattering phase shifts of the $\alpha\alpha$ system. The Coulomb potentials are constructed by folding the p-p Coulomb force with the proton densities of all the participating clusters. Since the use of the present $\alpha\alpha$ and αn interactions does not precisely reproduce the energies of the low-lying states of ^{9}Be as measured from the $\alpha\alpha n$ threshold, we introduce an additional phenomenological $\alpha\alpha n$ three-body force so as to fit the observed energies of the $3/2^-_1$ ground state and $5/2^-_1$, $1/2^-_1$ and $1/2^+_1$ excited states in ^{9}Be. The parameters of this $\alpha\alpha n$ three-body force are listed in Ref. 28). This $V_{\alpha\alpha}$ potential is applied to the three-body calculation of the $\alpha\alpha p$ system, and the energy of the ground state reproduces the observed data well.

3.2. *Charge symmetry breaking interaction*

It is beyond the scope of this work to explore the origin of the CSB interaction. We employ here the following phenomenological CSB interaction with a one-range Gaussian form:

$$V^{\mathrm{CSB}}_{\Lambda N}(r) = -\frac{\tau_z}{2}\Big[\frac{1+P_r}{2}(v_0^{\mathrm{even,CSB}} + \boldsymbol{\sigma}_\Lambda\cdot\boldsymbol{\sigma}_N v^{\mathrm{even,CSB}}_{\sigma_\Lambda\cdot\sigma_N})\, e^{-\beta_{\mathrm{even}}\, r^2}$$

$$+ \frac{1-P_r}{2}(v_0^{\rm odd,CSB} + \boldsymbol{\sigma}_\Lambda \cdot \boldsymbol{\sigma}_N v_{\sigma_\Lambda \cdot \sigma_N}^{\rm odd,CSB})\, e^{-\beta_{\rm odd}\, r^2} \Big], \tag{3·1}$$

which includes spin-independent and spin-spin parts. The range parameter $\beta_{\rm even}$ is taken to be 1.0 fm^{-2}. The parameters $v_0^{\rm even}$ and $v_{\sigma\sigma}^{\rm even}$ are determined phenomenologically to reproduce the values of $\Delta_{\rm CSB}$ derived from the Λ binding energies of the 0^+ and 1^+ states in the four-body calculation of ${}^{4}_{\Lambda}$H (${}^{4}_{\Lambda}$He). Then, we obtain $v_0^{\rm even,CSB} = 8.0$ MeV and $v_{\sigma\sigma}^{\rm even,CSB} = 0.7$ MeV.

In order to extract information about the odd-state part of CSB, it is necessary to study iso-multiplet hypernuclei in the p-shell region. A suitable system for such a study is ${}^{7}_{\Lambda}$He, in which the core nucleus ^{6}He is in a bound state. The JLab E01-011 experiment measured the ^{7}Li $(e, e'K^+){}^{7}_{\Lambda}$He reaction and reported the binding energy of the ${}^{7}_{\Lambda}$He ground state to be $5.68 \pm 0.03 \pm 0.25$ MeV for the first time.[16),17)] The present experimental data has a large systematic error, which is of the same order as the discussed CSB effect. They measured the same reaction with the improved calibration in the JLab E05-115 experiment[29)] and a more accurate result will be obtained in the near future. Before the final experimental result of the ${}^{7}_{\Lambda}$He is obtained, we will use our calculated binding energy of ${}^{7}_{\Lambda}$He, $B_\Lambda = 5.36$ MeV which locates around the limit of the current experimental error, to tune the strength and range of the odd-state. The range parameter $\beta_{\rm odd}$ is taken to be 1.5 fm. The strengths of $v_0^{\rm odd,CSB}$ and $v_{\sigma\sigma}^{\rm odd,CSB}$ are taken to be 16.0 MeV and 0.7 MeV, respectively. Using these potential parameters, the Λ-separation energy of the mirror Λ hypernucleus ${}^{7}_{\Lambda}$Be is 5.27 MeV, which also reproduces the observed data.

§4. Results

4.1. *Spin doublet states of $A = 10$ hypernuclei*

First, let us describe the level structures of ${}^{10}_{\Lambda}$B and ${}^{10}_{\Lambda}$Be obtained with the $\alpha + \Lambda + N + N$ four-body model, when the CSB interaction is not included. Calculations are performed for four-body bound states in these Λ hypernuclei.

In Figs. 2 and 3 and in Table I, we show the level structures of ${}^{10}_{\Lambda}$B and ${}^{10}_{\Lambda}$Be. In each figure, hypernuclear levels are shown in four columns in order to demonstrate separately the effects of the even-state and odd-state ΛN interactions, and also the SLS and ALS interactions. Even when the CSB interactions are switched on, their small contributions do not alter the features of these figures. Table I gives the calculated Λ binding energies and root mean square (r.m.s.) distances of subsystems in ${}^{10}_{\Lambda}$B and ${}^{10}_{\Lambda}$Be.

It is considered that the 1^--2^-_1 spin-doublet states in ${}^{10}_{\Lambda}$B and ${}^{10}_{\Lambda}$Be, and also the 2^-_2-3^- and 0^+-1^+ spin-doublet states in ${}^{10}_{\Lambda}$Be give useful information about the underlying spin dependence of the ΛN interaction. Note that the ΛN interaction used in the present calculations is identical to the one used in our previous analyses of the $T = 0$ spin-doublet state of ${}^{7}_{\Lambda}$Li[3)] and the $3/2^+$-$5/2^+$ spin-doublet states of ${}^{7}_{\Lambda}$He and ${}^{7}_{\Lambda}$Li with $T = 1$.[24)]

As shown in Fig. 2, we see that the resultant energy splitting of the 1^--2^-_1 states in ${}^{10}_{\Lambda}$B is 0.08 MeV, with combined contributions from the spin-spin, SLS and ALS

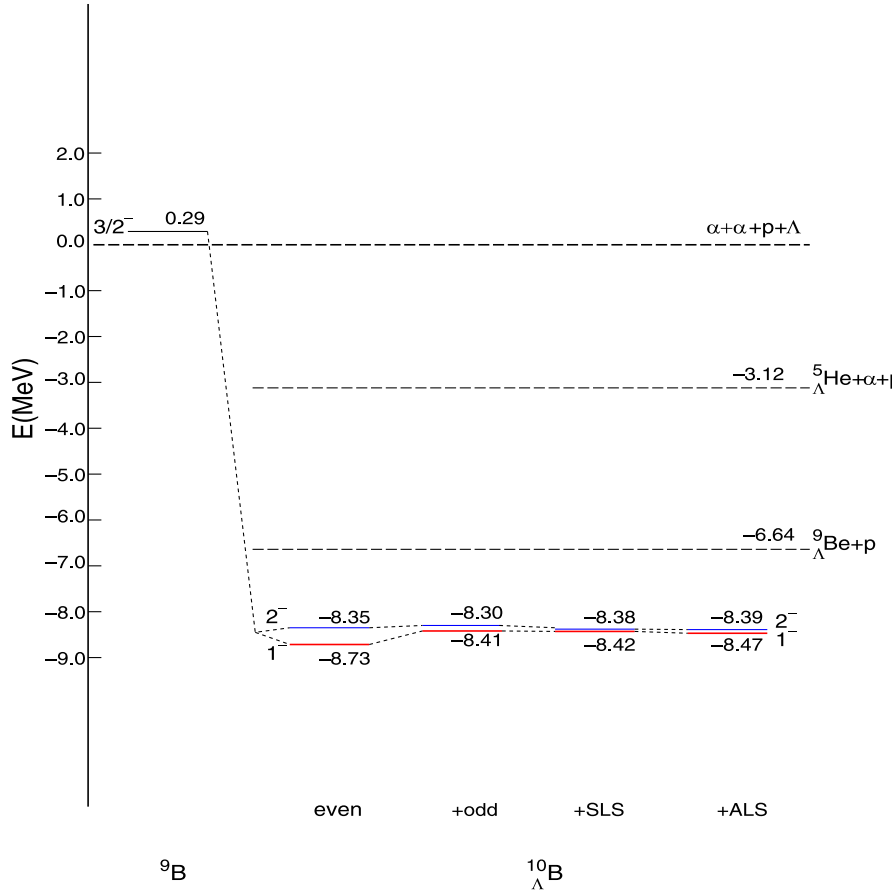

Fig. 2. (color online) Calculated energy levels of ^{9}B and $^{10}_{\Lambda}$B. The charge symmetry breaking potential is not included in $^{10}_{\Lambda}$B. The level energies are measured with respect to $\alpha + \alpha + \Lambda + p$ particle breakup threshold.

interactions. For the study of the ΛN spin-dependent interaction, in BNL-E930, they tried to measure the 1^{-}-2^{-}_{1} spin-doublet states in $^{10}_{\Lambda}$B using the ^{10}B$(K^{-}, \pi^{-}\gamma)$ reaction. However, no $M1$ transition between the ground-state doublet members $(2^{-}_{1} \to 1^{-})$ was observed. This measurement suggests the following two possibilities: The energy splitting between the 1^{-} and 2^{-}_{1} states is less than 100 keV and the γ ray cannot be observed, since the γ-ray detection efficiency drops rapidly below 100 keV. The other suggestion is that the 2^{-}_{1} state, which is dominantly produced by the $(K^{-}, \pi^{-}\gamma)$ reaction, is the ground state. Our result supports the former.

Next, let us see in more detail how the ΛN spin-spin interactions contribute to the 1^{-}-2^{-} doublets in $^{10}_{\Lambda}$B. The 1^{-} state is composed of $[K = 1(N\Lambda)_{s=0,1}]_{J=1^{-}}$ and $[K = 2(N\Lambda)_{s=1}]_{J=1^{-}}$, where K is the angular momentum and s is the spin of $N-\Lambda$ described in Eq. (2·3). Among these three components, $[K = 1(N\Lambda)_{s=0,1}]_{J=1^{-}}$ components are comparable to each other. On the other hand, the 2^{-}_{1} state is com-

posed of $[K = 1(N\Lambda)_{s=1}]_{J=2^-}$ and $[K = 2(N\Lambda)_{s=0,1}]_{J=2^-_1}$ components, where the $[K = 1(N\Lambda)_{s=1}]_{J=2^-_1}$ and $[K = 2(N\Lambda)_{s=1}]_{J=2^-_1}$ components are larger than the other one. $V_{\Lambda N}({}^1E)$ is more attractive than $V_{\Lambda N}({}^3E)$, when they are adjusted to reproduce the 0^+-1^+ splitting energy in ${}^4_{\Lambda}$H (${}^4_{\Lambda}$He). In ${}^{10}_{\Lambda}$B, this even-state interaction makes the 1^- state lower than the 2^-_1 state. The value obtained for the splitting energy is 0.38 MeV. This value is far larger than the above limitation of 100 keV suggested by the no γ-ray observation in BNL-E930. On the other hand, the calculated value of B_Λ in the ground state is 9.02 MeV, which is consistent with the experimental value of 8.89 ± 0.12 MeV within the error bar.

Next, when the odd-state interaction is switched on, the energy splitting is reduced to 0.11 MeV (see '+odd' column). The reason for this reduction is $V_{\Lambda N}({}^1O)$ being more repulsive than $V_{\Lambda N}({}^3O)$ as indicated in our analysis for the $1/2^+$-$3/2^+$ spin-doublet state in ${}^7_{\Lambda}$Li. Then, in ${}^{10}_{\Lambda}$B, the 1^- state including dominantly the ΛN spin-singlet component is pushed up more than the 2^-_1 state.

Moreover, we study the effects of the SLS and ALS interactions on 1^- and 2^-_1 doublet states. As shown in Fig. 2, the SLS works attractively for the 2^-_1 state because the contribution of the ΛN spin-triplet state is dominant in this state, while its contribution is very small to the 1^- state, which is dominated by the spin-singlet component. Thus, the 1^--2^-_1 splitting is found to be reduced by the SLS.

On the other hand, the ALS works significantly in the 1^- state, because the ALS acts between the spin= 0 and 1 ΛN components and both of them are included in the 1^- state. However, the ALS contribution is not significant in the 2^-_1 state, because this state is dominated by the spin = 1 ΛN component.

As a result of including both the spin-spin and spin-orbit terms, the energy splitting of the 1^--2^-_1 states of ${}^{10}_{\Lambda}$B leads to be 0.08 MeV. Then, we obtain the calculated value $B_\Lambda({}^{10}_{\Lambda}\mathrm{B}) = 8.76$ MeV which does not differ significantly from the experimental value, 8.89 ± 0.12 MeV.

We can see the same tendency in ${}^{10}_{\Lambda}$Be and the resultant energy splitting is 0.08 MeV, which is the same as that of ${}^{10}_{\Lambda}$B, as shown in Fig. 3. The calculated B_Λ value of the ground state is 8.94 MeV. As in the ${}^{10}_{\Lambda}$B case, this value is rather close to the experimental value $B_\Lambda({}^{10}_{\Lambda}\mathrm{Be}) = 9.11 \pm 0.22$ MeV. A more detailed discussion of the binding energies of ${}^{10}_{\Lambda}$B and ${}^{10}_{\Lambda}$Be with/without CSB interaction will appear in the next section. Next, let us discuss one more spin-doublet state, 2^-_2-3^-, in ${}^{10}_{\Lambda}$Be. The dominant component of the 2^-_2 (3^-) state is $[K = 2(N\Lambda)_{s=0}]_{J=2^-_2}$ ($[K = 2(N\Lambda)_{s=1}]_{J=3^-}$). Then, when we use our even-state interaction, the 2^-_2 state becomes lower than the 3^- state and the energy splitting is 0.43 MeV. When the odd-state interaction is included in the calculations of 2^-_2 and 3^- states, the energy of the 2^-_2 state is pushed up more than that of the 3^- state owing to the repulsive contribution of the $V^{(^1O)}_{\Lambda N}$ component and the energy splitting is 0.12 MeV. When the SLS interaction is added to the calculations of these states, the SLS contributes dominantly to the 3^- state. Finally, the repulsive ALS interaction, having the opposite sign of the SLS, contributes mainly to the 2^-_2 state including both the spin-singlet and spin-triplet states. As a result, we have 0.05 MeV for the 3^--2^-_2 doublet splitting.

Furthermore, above the 3^- and 2^-_2 states, we have the 0^+ and 1^+ states as bound

states, which is composed of $^9\mathrm{Be}(1/2^+) + \Lambda(0s_{1/2})$. In the core nucleus, ^{9}Be, the $1/2^+$ state is observed as the first excited state and is lower than the $5/2^-$ and $1/2^-$ excited states, despite the last neutron in this $1/2^+$ state presumably occupying the $1s_{1/2}$ orbit in the simple shell model configuration, whereas the next two excited states with negative parity would have $1p$-shell configurations. It is interesting to see that the order of the 3^-, 2^-_2, 0^+ and 1^+ states is reversed from ^{9}Be to $^{10}_{\Lambda}$Be. The $5/2^-$ state is composed of $^8\mathrm{Be}(2^+) + n(p_{1/2}, p3/2)$ and then there is a centrifugal barrier between $\alpha\alpha$ and a valence neutron, while the $1/2^+$ state does not have any barrier. Thus, it is considered that the $5/2^-$ state is more compact than the $1/2^+$ state. When a Λ particle adds into these states, we see that the energy gain is larger in the compactly coupled state ($5/2^-$) than in the loosely coupled state ($1/2^+$). Note that the same type of theoretical prediction was reported in our early work[2] for the $\alpha\alpha\alpha\Lambda$ four-body model of $^{13}_{\Lambda}$C, where the Λ particle is added to the compact bound state (3^-_1) and loosely bound state (0^+_2) in ^{12}C.

Let us discuss the energy splitting of these positive parity states. The dominant component of the 0^+ (1^+) is $[K = 0(N\Lambda)_{s=0}]_{0^+}$ ($[K = 0(N\Lambda)_{s=1}]_{1^+}$). Then, using the even state spin-spin interaction, the 0^+ state is lower than the 1^+ state and the energy splitting is 0.57 MeV. When the odd-state spin-spin interaction is employed, the energy of the 0^+ is pushed up more than that of the 1^+ state owing to the repulsive contribution of the $V^{(^1O)}_{\Lambda N}$ component and the energy splitting is 0.26 MeV. Since these two states are composed of $^9\mathrm{Be}(1/2^+) + \Lambda(0s_{1/2})$ as mentioned earlier, the relative angular momenta between composed particles are almost s-wave; then the spin-orbit contribution for these doublets is very small. As shown in Fig. 3, we see that the contributions of SLS and ALS for these doublets are small. Thus, we have 0.2 MeV finally for this positive parity doublet.

In Fig. 3, we found that the energy splittings of the negative parity doublets are less than 0.1 MeV, while that of the positive parity state is much larger. The reason for this is as follows: The αN spin-orbit interaction makes the 2^- state lower than the 1^- state. On the other hand, the ΛN spin-spin interaction makes the 1^- state lower than the 2^- state. Owing to the cancellation between the αN spin-orbit interaction and ΛN spin-spin interaction, we have less than 0.1 MeV splitting energy. To investigate the effect of the αN spin-orbit interaction for the 1^--2^- doublet state, as a trial, we turn off the αN spin-orbit term. In this case, we use ΛN even- and odd-state spin-spin forces. Then, the energy splitting is obtained to be 0.27 MeV owing to the even- and odd-state spin-spin forces. This value is similar to that of the 0^+-1^+ state. Thus, we find that αN spin-orbit force contributes to the energy splitting of the ground state doublet.

On the other hand, in the case of the 0^+ and 1^+ states, the αN spin-orbit contribution to this energy splitting is significantly small, because the composed particles α and N are in the s-state relatively. As a result, we obtain a pure contribution of the spin-spin ΛN interaction for the energy splitting of the 0^+ and 1^+ states, 0.2 MeV.

If the experiment of $^{10}\mathrm{B}(e, e'K^+)^{10}_{\Lambda}$Be at JLab can be performed within 200 keV resolution in the future, it might be possible to observe the energy of these two

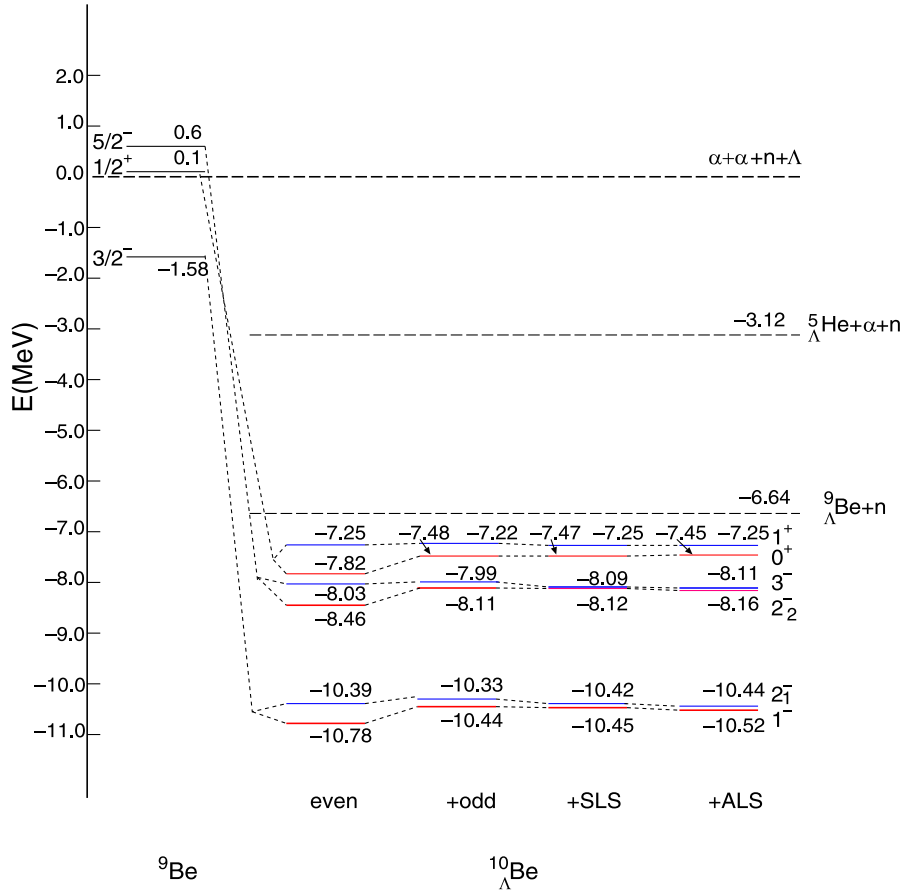

Fig. 3. (color online) Calculated energy levels of ^{9}Be and ${}^{10}_{\Lambda}$Be. The charge symmetry breaking potential is not included in ${}^{10}_{\Lambda}$Be. The level energies are measured with respect to $\alpha+\alpha+\Lambda+n$ particle breakup threshold.

positive states.

It is interesting to explore the glue like role of the Λ particle in ${}^{10}_{\Lambda}$B and ${}^{10}_{\Lambda}$Be. Although the ground state of ^{9}B is unbound, the corresponding states $(1^-, 2^-_1)$ in Λ hypernucleus become bound by $1.7-2.0$ MeV owing to the addition of a Λ particle. On the other hand, the ground state of the core nucleus ^{9}Be is bound by 1.58 MeV with respect to the $\alpha+\alpha+n$ three-body threshold. Owing to an additional Λ particle, the corresponding ground state of ${}^{10}_{\Lambda}$Be becomes rather deeply bound by ~ 4 MeV. Furthermore, the $5/2^-$ resonant state of ^{9}Be becomes bound (3^- and 2^-_2 in ${}^{10}_{\Lambda}$Be) by ~ 1.2 MeV owing to the presence of the Λ particle. In addition, when a Λ particle is added to the $1/2^+$ state of ^{9}Be, the 0^+ and 1^+ states of ${}^{10}_{\Lambda}$Be become weakly bound by less than 1.0 MeV.

In Table I, we list the calculated values of the r.m.s. radii between the composed particles $\bar{r}_{\alpha-\alpha}$, $\bar{r}_{\alpha-\Lambda}$, $\bar{r}_{\alpha-N}$ and $\bar{r}_{\Lambda-N}$ in our four-body model of ${}^{10}_{\Lambda}$B and ${}^{10}_{\Lambda}$Be.

Table I. Calculated energies of the low-lying states of (a) ${}^{10}_{\Lambda}$B and (b)${}^{10}_{\Lambda}$Be without the charge symmetry breaking potential, together with those of the corresponding states of ^{9}B and ^{9}Be, respectively. E stands for the total interaction energy among constituent particles. The energies in the parentheses are measured from the corresponding lowest particle-decay thresholds ${}^{9}_{\Lambda}$Be+N for ${}^{10}_{\Lambda}$B and ${}^{10}_{\Lambda}$Be. The calculated r.m.s. distances, $\bar{r}_{\alpha-\alpha}$, $\bar{r}_{\alpha-\Lambda}$ $\bar{r}_{\alpha-n}$, and $\bar{r}_{\Lambda-N}$ are also listed for the bound state.

(a)

	^{9}B($\alpha\alpha p$)	${}^{10}_{\Lambda}$B($\alpha\alpha\Lambda p$)	
J^π	$3/2^-$	1^-	2^-
E (MeV)	$+0.29$	-8.47	-8.39
$E^{\rm exp}$(MeV)	0.28		
		(-1.83)	(-1.75)
B_Λ(MeV)		8.76	8.67
$B_\Lambda^{\rm exp}$ (MeV)		8.89 ± 0.12	
$\bar{r}_{\alpha-\alpha}$(fm)		3.32	3.30
$\bar{r}_{\alpha-\Lambda}$(fm)		3.04	3.02
$\bar{r}_{\alpha-p}$(fm)		3.64	3.64
$\bar{r}_{\Lambda-p}$(fm)		3.86	3.87

(b)

	^{9}Be($\alpha\alpha n$)		${}^{10}_{\Lambda}$Be($\alpha\alpha\Lambda n$)					
J^π	$3/2^-$	$5/2^-$	1^-	2_1^-	2_2^-	3^-	0^+	1^+
E (MeV)	-1.58	0.60	-10.52	-10.44	-8.16	-8.11	-7.45	-7.25
$E^{\rm exp}$(MeV)	-1.58	0.85						
			(-3.88)	(-3.80)	(-1.52)	(-1.47)	(-0.81)	(-0.61)
B_Λ(MeV)			8.94	8.86	6.58	6.53	5.87	5.67
$B_\Lambda^{\rm exp}$ (MeV)			9.11 ± 0.22					
$\bar{r}_{\alpha-\alpha}$(fm)	3.68	-	3.27	3.26	3.29	3.24	3.78	3.76
$\bar{r}_{\alpha-\Lambda}$(fm)			3.02	3.00	3.02	3.00	3.31	3.30
$\bar{r}_{\alpha-n}$(fm)	4.56	-	3.52	3.51	3.56	3.56	4.95	5.04
$\bar{r}_{\Lambda-n}$(fm)			3.77	3.75	3.85	3.80	5.04	5.15

From the calculated rms radii, it is interesting to look at the dynamical change of the nuclear core ^{9}Be, which occurs owing to the addition of a Λ particle. The possibility of nuclear-core shrinkage owing to an addition of Λ-particle was originally pointed out in Ref. 30) by using the $\alpha x \Lambda$ three-cluster model ($x = n, p, d, t,{}^{3}$He, and α) for p-shell Λ hypernuclei. As for the hypernucleus ${}^{7}_{\Lambda}$Li, the prediction of some 20% shrinkage, in Ref. 30) and in an updated calculation,[31] was confirmed by experiment.[32] As shown in Table I, the rms distance $\bar{r}_{\alpha-\alpha}$ between two α clusters and $\bar{r}_{\alpha-N}$ between α and a nucleon are reduced by $12-17\%$ with the addition of a Λ particle.

As shown in Table I, the values of $\bar{r}_{\alpha-N}$ in these systems are larger than those of $\bar{r}_{\alpha-\Lambda}$, indicating that the distributions of valence nucleons have longer-ranged tails than those of the Λ's in the respective systems. In particular, $\bar{r}_{\alpha-N}$ in the 0^+ and 1^+ states are much larger, around 5 fm, than those of the other states. Then, it is expected that these positive parity states have neutron halos.

In order to see the structures of these systems visually, in Fig. 4, we draw the density distributions of the Λ (dashed curve) and valence neutrons (solid curve) of

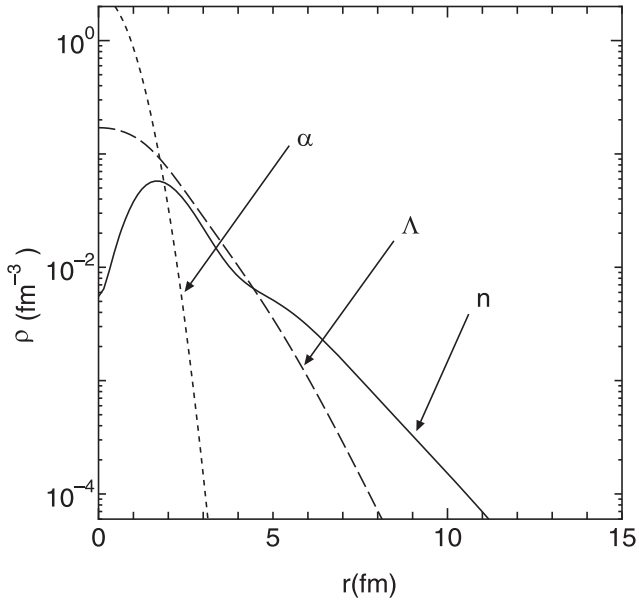

Fig. 4. Calculated density distributions of α, a Λ particle and a valence nucleon for the 0^+ state of ${}^{10}_{\Lambda}$Be without a charge symmetry breaking potential.

0^+ state of ${}^{10}_{\Lambda}$Be. For comparison, a single-nucleon density in the α core is also shown by the dotted curve. One finds that we have a long-range neutron density as shown in Fig. 4.

In addition, we show the density distributions of the 1^- state of ${}^{10}_{\Lambda}$Be and ${}^{10}_{\Lambda}$B in Fig. 5. In each case, the density distribution of a Λ particle has a shorter-ranged tail than that of a valence nucleon, but is extended significantly far away from the α core, which can be thought of as three layers of matter composed of two α clusters, a Λ particle, and a nucleon.

4.2. *Charge symmetry breaking effects*

Let us focus on the ground states in ${}^{10}_{\Lambda}$Be and ${}^{10}_{\Lambda}$B. It is likely that the CSB interaction affects the binding energies of these isodoublet hypernuclei.

In §3.2, we introduce the phenomenological CSB potential with the central-force component only. The CS part of the two-body ΛN interaction is fixed to reproduce the average energy spectra of ${}^{4}_{\Lambda}$H and ${}^{4}_{\Lambda}$He, and then the even-state part of the CSB interaction is adjusted to reproduce both the energy levels of these hypernuclei. In our previous work,[24] this CSB interaction was applied to calculations of the binding energies of the $A = 7$ isotriplet hypernuclei, ${}^{7}_{\Lambda}$He, ${}^{7}_{\Lambda}$Li($T = 1$), and ${}^{7}_{\Lambda}$Be. Here, the CSB interaction works repulsively (+0.20 MeV) and attractively (−0.20 MeV), in ${}^{7}_{\Lambda}$He and ${}^{7}_{\Lambda}$Be, respectively. As a result, our calculated values do not reproduce the observed B_Λs between ${}^{7}_{\Lambda}$He and ${}^{7}_{\Lambda}$Be. Furthermore, in Ref. 24), we pointed out that the same phenomena was seen in the energy difference of the $T = 1/2$ isodoublet $A = 8$ hypernuclei (${}^{8}_{\Lambda}$Li, ${}^{8}_{\Lambda}$Be): The agreement to the observed data of the energy difference becomes worse by introducing the CSB Λ-t(^{3}He) interaction.

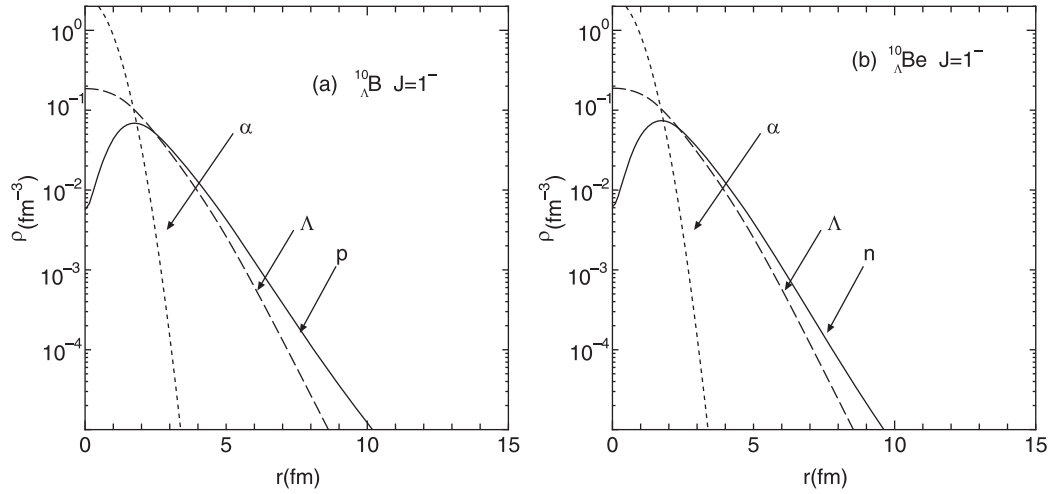

Fig. 5. Calculated density distributions of α, a Λ particle and a valence nucleon for (a)$^{10}_{\Lambda}$B and (b)$^{10}_{\Lambda}$Be without a charge symmetry breaking potential.

Let us discuss the energy difference of $^{10}_{\Lambda}$Be and $^{10}_{\Lambda}$B using the even-state CSB interaction employed in $A = 7$ hypernuclei. First, in Fig. 6(a), we show the energy spectra of the $A = 10$ hypernuclei calculated without a CSB interaction. The calculated B_Λ values of $^{10}_{\Lambda}$Be and $^{10}_{\Lambda}$B are 8.94 and 8.76 MeV, respectively.

Second, we turn on the even-state CSB interaction. In Fig. 6(b), it is found that the CSB interaction works repulsively by +0.1 MeV and attractively by −0.1 MeV in $^{10}_{\Lambda}$Be and $^{10}_{\Lambda}$B, respectively. This behavior is similar to the case of $A = 4$ and 7 hypernuclei.

Let us consider the energies of these $A = 10$ hypernuclei more in detail. In the case of $^{10}_{\Lambda}$Be, the CSB interaction between the Λ particle and a valence neutron works repulsively and the ground-state binding energy leads to $B_\Lambda = 8.83$ MeV, which is less bound by 0.1 MeV than the value without the CSB effect. In $^{10}_{\Lambda}$B, the CSB interaction contributes attractively by 0.1 MeV, and the binding energy of the ground state is $B_\Lambda = 8.85$ MeV, which is close to the experimental data. In order to see the CSB effect in the $A = 10$ hypernuclei more clearly, let us evaluate the difference between the calculated B_Λ values for $^{10}_{\Lambda}$Be and $^{10}_{\Lambda}$B; $\Delta B_\Lambda^{\rm cal} = B_\Lambda^{\rm cal}(^{10}_{\Lambda}{\rm B}) - B_\Lambda^{\rm cal}(^{10}_{\Lambda}{\rm Be}) = -0.18$ MeV without CSB, which is in good agreement with the experimental value, $\Delta B_\Lambda^{\rm exp} = B_\Lambda^{\rm exp}(^{10}_{\Lambda}{\rm B}) - B_\Lambda^{\rm exp}(^{10}_{\Lambda}{\rm Be}) = -0.22 \pm 0.25$ MeV. By switching on the even-state CSB interaction, the value obtained for $\Delta B_\Lambda^{\rm cal} = 0.02$ MeV moves away from the central value of the data, −0.22 MeV.

In this way, we find that if we introduce a phenomenological ΛN CSB interaction, the binding energies of $A = 7, 8, 10$ Λ hypernuclei become inconsistent with the observed data.

We can also discuss the CSB effects in s-shell and p-shell Λ hypernuclei from the experimental data. The observed binding energy of $^{4}_{\Lambda}$He is larger by 0.35 MeV than that of $^{4}_{\Lambda}$H. Namely, it seems that $p\Lambda$ interaction is more attractive than $n\Lambda$ interaction by the CSB effect. On the other hand, the observed binding energies of

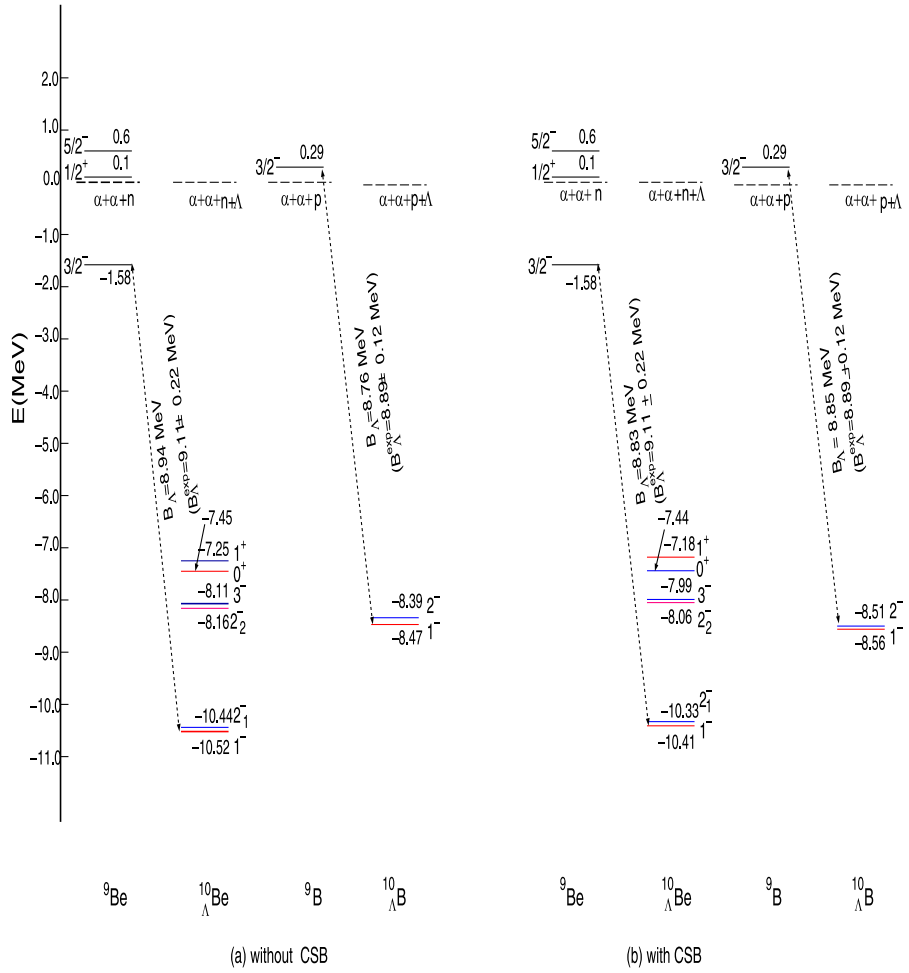

Fig. 6. (color online) Calculated energy levels of ^{9}Be, ${}^{10}_{\Lambda}$Be, ^{9}B, and ${}^{10}_{\Lambda}$B with spin-spin and spin-orbit ΛN interactions. The even-state CSB potential is not included in the calculated energies of ${}^{10}_{\Lambda}$Be and ${}^{10}_{\Lambda}$B of (a), and included in those of (b). The energies are measured from the particle breakup threshold.

${}^{7}_{\Lambda}$He, ${}^{8}_{\Lambda}$Li and ${}^{10}_{\Lambda}$Be are larger than those of ${}^{7}_{\Lambda}$Be, ${}^{8}_{\Lambda}$Be and ${}^{10}_{\Lambda}$B. This means that the $n\Lambda$ interaction is more attractive than the $p\Lambda$ interaction.

One possibility to solve this contradiction is to reinvestigate the experimental data, especially those of the s-shell Λ hypernuclei ${}^{4}_{\Lambda}$H and ${}^{4}_{\Lambda}$He. In fact, it is planned to measure the M1 transition from the 1^+ state to the 0^+ state in ${}^{4}_{\Lambda}$He at the E13 J-PARC project[33] and to measure the Λ separation energy of the 0^+ state in ${}^{4}_{\Lambda}$H at Maintz and JLab.

One of the candidates for solving the contradiction is simply to introduce the odd-state CSB interaction with an opposite sign to the even-state CSB interaction. The odd-state CSB interaction is negligible in s-shell Λ hypernuclei but significant in p-shell Λ hypernuclei.

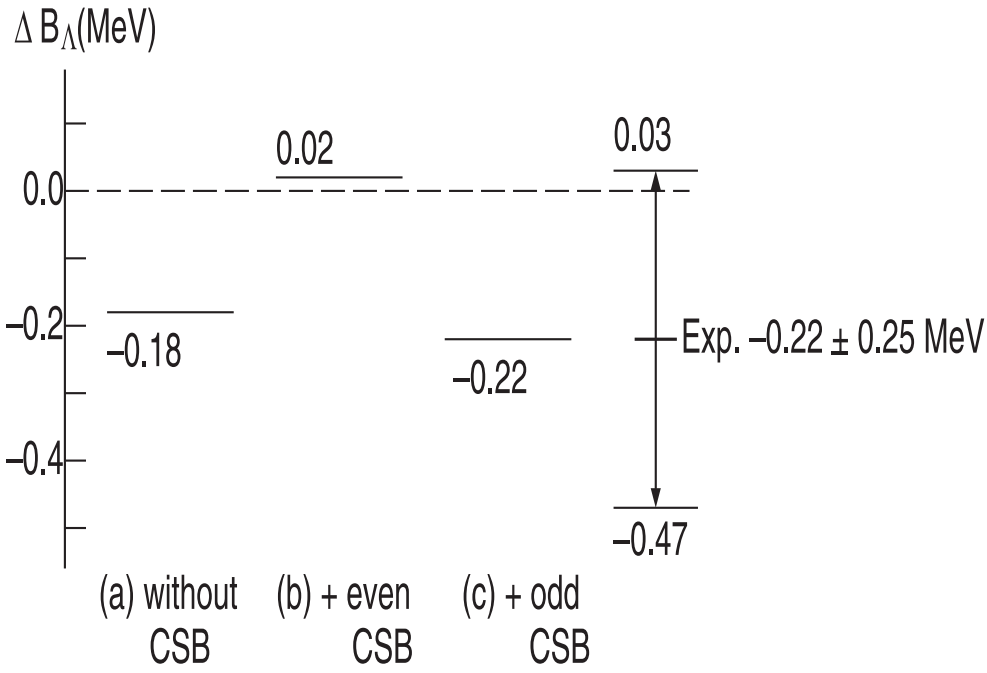

Fig. 7. Calculated energy difference of ${}^{10}_{\Lambda}$Be and ${}^{10}_{\Lambda}$B, $\Delta B_\Lambda({}^{10}_{\Lambda}\mathrm{B}) - B_\Lambda({}^{10}_{\Lambda}\mathrm{Be})$, (a) without CSB, (b) with even-state CSB, and (c) with both even- and odd-state CSB interactions.

In Ref. 24), we pointed out that in order to reproduce the data of these $A = 8$ hyernuclei, it was necessary that the sign of the odd-state CSB interaction be opposite to that of the even state CSB interaction.[24)]

It is expected that such an odd-state CSB interaction plays the same role in the $A = 7$ and 10 hypernuclei. Here, we show the results of ${}^{10}_{\Lambda}$Be and ${}^{10}_{\Lambda}$B without the CSB and with even-state CSB chosen to reproduce the observed binding energies of ${}^{4}_{\Lambda}$H and ${}^{4}_{\Lambda}$He, and with even- and odd-state CSB interactions. The odd-state CSB interaction is introduced with an opposite sign to that the even-state part, but whose contributions in the ${}^{4}_{\Lambda}$H and ${}^{4}_{\Lambda}$He are negligible. Their potential parameters, strengths and ranges are fixed to reproduce our calculated B_Λ for ${}^{7}_{\Lambda}$He, 5.36 MeV. The detailed potential parameters are mentioned in §3.2.

Next, we apply the strong odd-state CSB interaction to level structures of ${}^{10}_{\Lambda}$Be and ${}^{10}_{\Lambda}$B. The calculated Λ-separation energies of the 1^- states for ${}^{10}_{\Lambda}$Be and ${}^{10}_{\Lambda}$B are 8.96 MeV and 8.74 MeV, respectively. Then, $\Delta B_\Lambda^{\mathrm{cal}} = -0.22$ MeV, which is in good agreement with $\Delta B_\Lambda^{\mathrm{exp}} = -0.22 \pm 0.25$. The binding energies of $A = 7$ and 10 Λ hypernulclei with and without CSB interaction are listed in Table II.

Three results of $A = 10$ hypernuclei are summarized in Fig. 7. Three results shown by solid lines are found to be within the experimental error bars. We see the deviation by 200 keV in the $\Delta B_\Lambda^{\mathrm{exp}}$ with and without the CSB interaction. Then, if high-resolution experiments can provide us new data for ${}^{10}_{\Lambda}$Be and ${}^{10}_{\Lambda}$B within 100 keV accuracy in the future, we can obtain information about the CSB interaction.

Table II. Calculated Λ separation energies of $A = 7$ and 10 Λ hypernuclei with and without CSB interactions. The $B_\Lambda^{\rm cal}({}^{10}_{\Lambda}{\rm Be}) - B_\Lambda^{\rm cal}({}^{10}_{\Lambda}{\rm B})$ and $\Delta B_\Lambda^{\rm exp} = B_\Lambda^{\rm exp}({}^{10}_{\Lambda}{\rm Be}) - B_\Lambda^{\rm exp}({}^{10}_{\Lambda}{\rm B})$ are listed here.

	without CSB	with even-state CSB	with even+odd-state CSB	Exp.
$B_\Lambda({}^{7}_{\Lambda}{\rm He})$	5.36	5.16	5.36	$5.68 \pm 0.03 \pm 0.25$[16),17)]
$B_\Lambda({}^{7}_{\Lambda}{\rm Li})$	5.28	5.29	5.28	5.26
$B_\Lambda({}^{7}_{\Lambda}{\rm Be})$	5.21	5.44	5.27	5.16 ± 0.08
$B_\Lambda({}^{10}_{\Lambda}{\rm Be})$	8.94	8.83	8.96	9.11 ± 0.22
$B_\Lambda({}^{10}_{\Lambda}{\rm B})$	8.76	8.85	8.74	8.89 ± 0.12
$\Delta B_\Lambda^{\rm cal}$	0.18	-0.02	0.22	0.22 ± 0.25

As shown in Table II and Fig. 7, the binding energies of $A = 7$ and 10 Λ hypernuclei without CSB interaction reproduce the all data. However, the even-state CSB interaction that reproduces the data of s-shell Λ hypernuclei ${}^{4}_{\Lambda}$H and ${}^{4}_{\Lambda}$He, leads to inconsistency in the binding energies of the p-shell Λ hyernuclei. As a trial, then, if we introduce a strong odd-state CSB interaction with an opposite sign of the even-state CSB interaction, we could reproduce the observed binding energies of $A = 7$ and 10 Λ hypernuclei. However, there is still room to discuss the validity of such a strong odd-state CSB interaction. For the CSB effect in light Λ hypernuclei, it is necessary to reinvestigate experimental data of s-shell Λ hypernuclei and p-shell Λ hypernuclei as mentioned before. In fact, it is planned to measure the M1 transition from the 1^+ state to the 0^+ state in ${}^{4}_{\Lambda}$He at the E13 J-PARC project[33)] and to measure the Λ separation energy of the 0^+ state in ${}^{4}_{\Lambda}$H at Maintz and JLab. From these measurements, we could conclude whether there exists a CSB effect in the binding energies of $A = 4$ hypernuclei. We need to wait for these data.

§5. Summary

We study the structure of hypernuclear isodoublet hypernuclei ${}^{10}_{\Lambda}$B and ${}^{10}_{\Lambda}$Be within the framework of the $\alpha + \alpha + \Lambda + N$ four-body model. In this model, it is important that all the two-body interactions among subunits (two α's, Λ and N) are chosen to reproduce the binding energies of all subsystems composed of two and three subunits. The ΛN interaction, which simulates ΛN scattering phase shifts of NSC97f, are adjusted to reproduce the observed data for the spin-doublets states 0^+-1^+ and $1/2^+$-$3/2^+$, of ${}^{4}_{\Lambda}$H and ${}^{7}_{\Lambda}$Li, respectively. Before discussing the major conclusion, we comment on our general viewpoint for effective interactions used in our cluster-model analyses. Our basic assumption in this work is that the ΛN-ΣN coupling interaction can be renormalized into the ΛN-ΛN interaction effectively. Note that our renormalizations into effective ΛN interactions are made to reproduce experimental values of binding energies of subunits such as ΛN, $\Lambda\alpha$, $\Lambda\alpha\alpha$ and so on. Here, we emphasized that the validity of nuclear models and effective interactions in them should be based on the consistency with experimental data: In our cluster-

model approach, the experimental data of the above hypernuclei are reproduced systematically with the use of our effective interactions.

The main conclusions can be summarized as follows:

(1) We calculated spin-doublet states of 1^--2^-_1 in ${}^{10}_{\Lambda}$B whose measurement was obtained in BNL930.[4] The calculated splitting energy is 0.08 MeV. This small value is less than the 0.1 MeV precision for detecting the M1 transition from the 2^- state to the 1^- state, which is consistent with the experimental fact of no observed γ-ray. Furthermore, we calculated the spin-doublets, 1^--2^-_1, 2^-_2-3^- and 0^+-1^+ states, of ${}^{10}_{\Lambda}$Be. The measurement for ${}^{10}_{\Lambda}$Be was performed at JLab and the analysis is in progress. The energy splittings of these states are predicted to be 0.08 MeV, 0.05 MeV and 0.2 MeV, respectively. Then, it would be difficult to observe the energy splittings for a negative parity, which are produced in the (K^-, π^-) experiment, although these energy splittings would be helpful for extracting information about the ΛN spin-dependent components.

(2) The effect of the gluelike role of the Λ particle can be demonstrated in ${}^{10}_{\Lambda}$B and ${}^{10}_{\Lambda}$Be. The ground state of ^{9}B is a resonant state. Owing to the presence of the Λ particle, the ground state of the resultant hypernucleus ${}^{10}_{\Lambda}$B becomes bound by about 2.0 MeV below the ${}^{9}_{\Lambda}$Be+p threshold. When the Λ particle is added to the bound ground state of ^{9}Be, the corresponding state of ${}^{10}_{\Lambda}$Be becomes bound more deeply by about 4 MeV below the ${}^{9}_{\Lambda}$Be+n threshold. Furthermore, by adding the Λ particle to the resonant state of ^{9}Be, $1/2^+$ and $5/2^-$, the corresponding states of ${}^{10}_{\Lambda}$Be become bound. In particular, we find that the order of the 3^-, 2^-_2, 0^+ and 1^+ states is reversed from ^{9}Be to ${}^{10}_{\Lambda}$Be. From the calculated values of the rms radii $\bar{r}_{\alpha-\alpha}$ and $\bar{r}_{\alpha-\Lambda}$ of ^{9}Be and ${}^{10}_{\Lambda}$Be, we find the shrinkage effect owing to the addition of Λ particle to the core nucleus.

Such an effect was already confirmed in the KEK-E419 experiment.[32] Another interesting feature seen in our result is the three-layer structure of the matter distributions in isodoublet hypernuclear states, being composed of a 2α core, a Λ particle, and a nucleon. Also, we have neutron halo structures for the 0^+ and 1^+ states.

(3) The charge symmetry breaking effects in ${}^{10}_{\Lambda}$Be and ${}^{10}_{\Lambda}$B are investigated quantitatively on the basis of the phenomenological CSB interaction, which describes the experimental energy difference between $B_\Lambda({}^{4}_{\Lambda}\mathrm{H})$ and $B_\Lambda({}^{4}_{\Lambda}\mathrm{He})$, Δ_{CSB}. We introduced $\Delta B_\Lambda = B_\Lambda({}^{10}_{\Lambda}\mathrm{Be}) - B_\Lambda({}^{10}_{\Lambda}\mathrm{B})$, and obtained a $\Delta B^{\mathrm{cal}}_\Lambda$ range of -0.02–0.22 MeV without and with the CSB interaction, which is in agreement with the observed $\Delta B^{\mathrm{exp}}_\Lambda$ within a large error bar.

In order to elucidate the CSB effects in light hypernuclei, it is necessary to have precise data for ${}^{4}_{\Lambda}$H, ${}^{4}_{\Lambda}$He, ${}^{7}_{\Lambda}$He, ${}^{7}_{\Lambda}$Li ($T = 1$), ${}^{7}_{\Lambda}$Be, ${}^{10}_{\Lambda}$Be and ${}^{10}_{\Lambda}$B. The calculated Λ separation energies of p-shell hypernuclei became inconsistent with the observed data when we use the even-state CSB interaction to reproduce the observed data of the s-shell Λ hypernuclei ${}^{4}_{\Lambda}$H and ${}^{4}_{\Lambda}$He.

In this contradictory situation, one possibility is to reinvestigate the experimental data, especially those of ${}^{4}_{\Lambda}$H and ${}^{4}_{\Lambda}$He. At J-PARC, it is planned to measure the M1 transition from the 1^+ state to the 0^+ state in ${}^{4}_{\Lambda}$He at the E13 J-PARC project[33] and to measure the Λ separation energy of the 0^+ state in ${}^{4}_{\Lambda}$H at Mainz and JLab. From these measurements, we can investigate the interesting issue of whether there is

a CSB effect in the binding energies of ${}^{4}_{\Lambda}$He and ${}^{4}_{\Lambda}$H. Furthermore, these experimental results must affect the discussion of CSB effect in p-shell Λ hypernuclei.

As a working assumption to explain the CSB effects in both $A = 4$ and p-shell systems, we have introduced the extremely repulsive odd-state CSB interaction to cancel out the even-state CSB contributions. Even if this assumption works well, it is an open problem to elucidate the physical reality for it. To find the effects of the odd-state CSB in $A = 10$ hypernuclei, we need data with 0.1 MeV resolution. In the case of ${}^{10}_{\Lambda}$B, we propose to perform the experiment ^{10}B $(K^-, \pi^-)^{10}_{\Lambda}$B at J-PARC in the future. In the case of ${}^{10}_{\Lambda}$Be, the experiment of ^{10}B $(e, e'K^+)^{10}_{\Lambda}$Be at JLab was carried out and analysis is in progress. We hope to have the Λ separation energy for this hypernucleus with a 0.1 MeV resolution.

Acknowledgements

The authors thank Professors O. Hashimoto, H. Tamura, S. N. Nakamura, T. Motoba, B. F. Gibson and D. J. Millener for helpful discussions. This work was supported by Grants-in-Aid for Scientific Research from Monbukagakusho of Japan (21540288 and 20105003). The numerical calculations were performed at the Yukawa Institute Computer Facility HITACHI-SR16000 and KEK-SR16000.

References

1) E. Hiyama, Y. Kino and M. Kamimura, Prog. Part. Nucl. Phys. **51** (2003), 223.
2) E. Hiyama, M. Kamimura, T. Motoba, T. Yamada and Y. Yamamoto, Phys. Rev. Lett. **85** (2000), 270.
3) E. Hiyama, Y. Yamamoto, Th. A. Rijken and T. Motoba, Phys. Rev. C **74** (2006), 054312.
4) H. Tamura et al., Nucl. Phys. A **754** (2005), 58.
5) D. J. Millener, Lecture Notes in Phys. **724** (2007), 31; Nucl. Phys. A **804** (2008), 84.
6) D. J. Millener, Nucl. Phys. A **835** (2010), 11.
7) R. H. Dalitz and F. Von Hippel, Phys. Lett. **10** (1964), 153.
8) S. A. Coon and P. C. McNamee, Nucl. Phys. A **322** (1979), 267.
9) A. R. Bodmer and Q. N. Usmani, Phys. Rev. C **31** (1985), 1400.
10) P. M. M. Maessen, Th. A. Rijken and J. de Swart, Phys. Rev. C **40** (1986), 2226.
11) Th. A. Rijken, V. G. J. Stoks and Y. Yamamoto, Phys. Rev. C **59** (1999), 21.
12) A. Nogga, H. Kamada and W. Glöckle, Phys. Rev. Lett. **88** (2002), 172501.
13) R. H. Dalitz, R. C. Herndon and Y. C. Tang, Nucl. Phys. B **47** (1972), 109.
14) A. Gal, Adv. Nucl. Sci. **8** (1977), 1.
15) B. F. Gibson and E. V. Hungerford III, Phys. Rep. **257** (1995), 349.
16) O. Hashimoto et al., J. Phys.: Conf. Ser. **312** (2011), 022015.
17) JLab E01-011 collaboration, to be submitted in Phys. Rev. Lett.
18) Y. Zhang, E. Hiyama and Y. Yamamoto, Nucl. Phys. A **881** (2012), 288.
19) S. Saito, Prog. Theor. Phys. **41** (1969), 705.
20) M. Kamimura, Phys. Rev. A **38** (1988), 621.
21) H. Kameyama, M. Kamimura and Y. Fukushima, Phys. Rev. C **40** (1989), 974.
22) V. I. Kukulin, V. N. Pomerantsev, Kh. D. Razikov, V. T. Voronchev and G. G. Ryzhinkh, Nucl. Phys. A **586** (1995), 151.
23) H. Kanada, T. Kaneko, S. Nagata and M. Nomoto, Prog. Theor. Phys. **61** (1979), 1327.
24) E. Hiyama, Y. Yamamoto, T. Motoba and M. Kamimura, Phys. Rev. C **80** (2009), 054321.
25) M. N. Nagels, T. A. Rijken and J. J. deSwart, Phys. Rev. D **15** (1977), 2547; Phys. Rev. D **20** (1979), 1633.
26) E. Hiyama, M. Kamimura, T. Motoba, T. Yamada and Y. Yamamoto, Prog. Theor. Phys. **97** (1997), 881.
27) A. Hasegawa and S. Nagata, Prog. Theor. Phys. **45** (1971), 1786.

28) E. Hiyama, M. Kamimura, Y. Yamamoto and T. Motoba, Phys. Rev. Lett. **104** (2010), 212502.
29) O. Hashimoto, S. N. Nakamura, L. Tang, J. Reinhold et al., JLab E05-115 proposal, "Spectroscopic investigation of hypernuclei in the wide mass region using the $(e, e'K^+)$ reaction" (2005).
30) T. Motoba, H. Bando and K. Ikeda, Prog. Theor. Phys. **70** (1983), 189.
T. Motoba, H. Bando, K. Ikeda and T. Yamada, Prog. Theor. Phys. Suppl. No. 81 (1985), 42.
31) E. Hiyama, M. Kamimura, K. Miayazaki and T. Motoba, Phys. Rev. C **59** (1999), 2351.
32) K. Tanida et al., Phys. Rev. Lett. **86** (2001), 1982.
33) H. Tamura et al., J-PARC proposal on 'γ-ray spectroscopy of light hyprnuclei' E13.